

Vibha Vansola, Reetuparna Ghosh, Sylvia Badwar, Bioletty Mary Lawriniang, Arjun Gopalakrishna, Haladhara Naik\*, Yeshwant Naik, Niles Subhash Tawade, Suresh Chand Sharma, Jignesh Pravinchandra Bhatt, Shri Krishna Gupta, Shankar Sarode, Surjit Mukherjee, Nand Lal Singh, Pitambar Singh, and Ashok Goswami

# Measurement of $^{197}\text{Au}(\text{n},\gamma)^{198}\text{Au}$ reaction cross-section at the neutron energies of 1.12, 2.12, 3.12 and 4.12 MeV

DOI 10.1515/ract-2015-2431

Received April 27, 2015; accepted August 17, 2015; published online September 30, 2015

**Abstract:** The  $^{197}\text{Au}(\text{n},\gamma)^{198}\text{Au}$  reaction cross-sections at the neutron energies of 1.12, 2.12, 3.12 and 4.12 MeV were determined by using activation and off-line  $\gamma$ -ray spectrometric technique. The mono-energetic neutron energies of 1.12–4.12 MeV were generated from the  $^7\text{Li}(\text{p},\text{n})$  reaction by using the proton energies of 3 and 4 MeV from the folded tandem ion beam accelerator (FOTIA) at BARC as well as 5 and 6 MeV from the Pelletron facility at TIFR, Mumbai. The  $^{115}\text{In}(\text{n},\gamma)^{116m}\text{In}$  reaction cross-section was used as the neutron flux monitor. The  $^{197}\text{Au}(\text{n},\gamma)^{198}\text{Au}$  reaction cross-section at the neutron energies of 3.12 and 4.12 MeV are reported for the first time. The  $^{197}\text{Au}(\text{n},\gamma)^{198}\text{Au}$  reaction cross-sections at 1.12 and 2.12 MeV are close to the literature data of in between neutron energies. The  $^{197}\text{Au}(\text{n},\gamma)^{198}\text{Au}$  cross-section was also calculated theoretically by using the computer code TALYS

1.6 and found to be higher than the experimental data of present work and literature data within the neutron energies of 0.8 to 4 MeV.

**Keywords:**  $^{197}\text{Au}(\text{n},\gamma)^{198}\text{Au}$  reaction cross-section, off-line  $\gamma$ -ray spectrometric technique,  $^{115}\text{In}(\text{n},\gamma)^{116m}\text{In}$  reaction monitor, TALYS calculation.

## 1 Introduction

For the determination of neutron activation cross-section at low neutron energy,  $^{197}\text{Au}(\text{n},\gamma)$  reaction cross-section is used as the neutron flux monitor. The  $^{197}\text{Au}(\text{n},\gamma)$  reaction cross-section at thermal neutron energy is known very accurately based on the evaluation and compilation of Mughabghab et al [1]. However, the reactor neutron has a spectrum within energy of thermal to 15 MeV. If it is desired to use the  $^{197}\text{Au}(\text{n},\gamma)$  reaction as a flux monitor at higher neutron energy then it is necessary to know the  $^{197}\text{Au}(\text{n},\gamma)$  reaction cross-section accurately at different neutron energies. In earlier days, it was difficult to obtain a mono-energetic neutron source with sufficient flux, except for the neutron energy of 2.45 MeV from the D + D reaction and of 14.8 MeV from the T + D reaction. However, in recent years mono-energetic neutrons from different reactions with good flux have become available. Among them,  $^7\text{Li}(\text{p},\text{n})$  reaction is a good mono-energetic neutron source within the proton energy of 6 MeV.

Sufficient  $^{197}\text{Au}(\text{n},\gamma)$  reaction cross-section data within the neutron energy range of 0.025 eV to 3 MeV and at 14.7 have been compiled in the EXFOR [2] based on the experimental data of various authors [3–16]. The  $^{197}\text{Au}(\text{n},\gamma)$  reaction cross-section was measured by various authors at the neutron energy of 0.025 eV [3, 4]. Similarly, data are available for the neutron energies of 0.024 to 3 MeV [5–13, 16] and at 14.7 MeV [14, 15]. Besides this, no experimental  $^{197}\text{Au}(\text{n},\gamma)$  reaction cross-section

\*Corresponding author: Haladhara Naik, Radiochemistry Division, Bhabha Atomic Research Centre, Mumbai-400085, India, e-mail: naikhbarc@yahoo.com

Nilesh Subhash Tawade, Ashok Goswami: Radiochemistry Division, Bhabha Atomic Research Centre, Mumbai-400085, India

Vibha Vansola, Surjit Mukherjee, Nand Lal Singh: Department of Physics, Faculty of Science, M. S. University, Baroda-390002, India

Reetuparna Ghosh, Sylvia Badwar, Bioletty Mary Lawriniang: Department of Physics, North Eastern Hill University, Shillong, Meghalaya-793022, India

Arjun Gopalakrishna: Medical Cyclotron Facility, Board of Radiation and Isotope Technology, Radiation Medicine Centre, Mumbai-400012, India

Yeshwant Naik: Product Development Division, Bhabha Atomic Research Centre, Mumbai-400085, India

Suresh Chand Sharma: Nuclear Physics Division, Bhabha Atomic Research Centre, Mumbai-400085, India

Jignesh Pravinchandra Bhatt, Shri Krishna Gupta, Shankar Sarode, Pitambar Singh: Ion Accelerator Development Division, Bhabha Atomic Research Centre, Mumbai-400085, India

data are available over neutron energy range of 3 to 14.7 MeV. In view of this, in the present work we have determined the reaction cross-section of  $^{197}\text{Au}$  with the neutron energies of 1.12, 2.12, 3.12 and 4.12 MeV by using the off-line gamma ray spectrometric technique. The  $^{197}\text{Au}(n,\gamma)^{198\text{g}}\text{Au}$  reaction cross-section was also calculated theoretically by using the computer code TALYS 1.6 [17] and compared with the experimental data from literature and present work.

## 2 Experimental details and calculations

For the measurement of  $^{197}\text{Au}(n,\gamma)^{198\text{g}}\text{Au}$  reaction cross-sections, experiments with four different neutron energies were carried out at two different places. The fast neutrons were produced from the  $^7\text{Li}(p,n)^7\text{Be}$  reaction by using the proton beam of 3, 4, 5 and 6 MeV. The Q-value for the  $^7\text{Li}(p,n)^7\text{Be}$  reaction to the ground state is  $-1.644$  MeV, whereas the first excited state is  $0.431$  MeV above the ground state leading to an average Q-value of  $-1.868$  MeV. The threshold value of the  $^7\text{Li}(p,n)$  reaction to the ground state of  $^7\text{Be}$  is  $1.881$  MeV. Thus for the proton energy of 3, 4, 5 and 6 MeV the resulting peak energy of the first group of neutrons ( $n_0$ ) would be 1.12, 2.12, 3.12 and 4.12 MeV, respectively. The corresponding neutron energy of the second group of neutrons ( $n_1$ ), for the first excited state of  $^7\text{Be}$ , will be 0.63, 1.63, 2.63 and 3.63 MeV, respectively [18–20]. This is because above the proton energy of 2.37 MeV, the  $n_1$  group of neutrons is also produced. However, the contribution from the  $n_1$  group neutrons is negligible within the proton energies of 6 MeV. For the proton energies of 4–6 MeV, the neutron spectrum consists of the full energy peak due to the  $^7\text{Li}(p,n)^7\text{Be}$  reaction and a continuum component attributable to the multi-body break up process, i.e.  $^7\text{Li}(p,n^3\text{He})\alpha$  ( $Q = -3.231$  MeV). However, the energies of the emitted neutrons under the main peak were estimated to be  $1.12 \pm 0.11$ ,  $2.12 \pm 0.15$ ,  $3.12 \pm 0.21$ , and  $4.12 \pm 0.32$  MeV, respectively.

The first experiment with the neutron energies of 1.12 and 2.12 MeV was performed using the folded tandem ion beam accelerator (FOTIA) at Van-de-Graff, BARC, Mumbai. A circular LiF pellet of 1 cm diameter and 3 mm thickness was used for neutron production. It was fixed on a stand inside in a zero degree angle of the beam exit window. A beam collimator of 10 mm diameter was used before the target. The current of incident proton beam during the irradiations was 100 nA for both 3 and 4 MeV. The

3 mm thick LiF pellet is sufficient to stop the proton beam of 3 and 4 MeV. About 52.7 to 59.1 mg of Au metal foil with purity  $\sim 99.99\%$  was wrapped with 0.025 mm thick Al foil. Similarly, 98.8 to 163.7 mg of In metal foil was also wrapped with 0.025 mm thick Al foil to prevent contamination from one another. The  $^{115}\text{In}(n,\gamma)^{116\text{m}}\text{In}$  reaction of the In metal foil was used as neutron flux monitor. Two sets of Al wrapped Au and In metal samples stack were made for two different irradiations. The Au-In stack was wrapped with additional Al foil and kept at a distance of 3 mm behind the LiF target. The stacks of samples were irradiated one set at a time with the neutron beam energies of 1.12 and 2.12 MeV, for 8.6 h and 5.6 h, respectively.

The second experiment was performed using the 14 UD BARC-TIFR Pelletron facility at TIFR, Mumbai with neutron energies of 3.12 and 4.12 MeV [21]. They were generated from the  $^7\text{Li}(p,n)^7\text{Be}$  reaction by using the proton energies of 5 and 6 MeV. The current of incident proton beam during the irradiations was 50 nA at 5 MeV and 60 nA at 6 MeV. These runs were carried out at 6 m height above the analysing magnet of the Pelletron facility to utilize the maximum proton current from the accelerator [21]. At this port, the terminal voltage is regulated by generating voltage mode (GVM) by using a terminal potential stabilizer. Furthermore, we use a beam collimator of 6 mm diameter before the target. The lithium foil was made up of natural lithium with thickness  $3.7\text{ mg/cm}^2$ , sandwiched between two tantalum foils of different thicknesses. The front tantalum foil facing the proton beam was the thinnest one ( $3.9\text{ mg/cm}^2$ ), in which the degradation of proton energy is 50–85 keV [22]. On the other hand, the back tantalum foil (beam stopper) was thicker (0.025 mm), which is used to stop the proton beam. For each irradiation, separate samples were made by packing 59–59.4 mg of Au metal foil wrapped with 0.025 mm thick aluminium foil. Similarly, 58.1–64.3 mg of In metal foil was also wrapped separately with 0.025 mm thick Al foil. Then two different sets of Al-wrapped Au and In metal stacks were prepared for different irradiations at neutron energies of 3.12 and 4.12 MeV, respectively. The individual stacks of Au-In samples were additionally wrapped with two different Al foils. The Au-In stack was mounted at zero degree angle with respect to the proton beam direction at a distance of 2.1 cm behind the Ta-Li-Ta stack [21]. A schematic diagram of the Ta-Li-Ta stack and of the Au-In stack is given in Figure 1. The samples were irradiated one set at a time with the neutron beam energies of 3.12 and 4.12 MeV. The irradiation time was 11.8 h for the neutron energy of 3.12 MeV and 13.4 h for 4.12 MeV. The neutron background during and before experiment was also

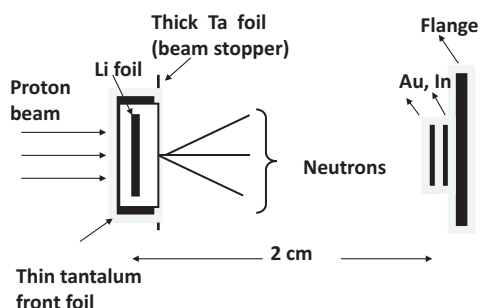


**Fig. 1:** Schematic diagram showing the arrangement used for neutron irradiation.

tested by keeping an inactive Au foil outside the irradiation chamber and was found to be absent.

In all those above experiments, the irradiated samples of Au and In were cooled for 2.3–19 h and 0.7–1.25 h, respectively. Then the  $\gamma$ -ray counting of the samples was done by using pre-calibrated  $80\text{ cm}^3$  HPGe detector couple to a PC based 4094 channel analyser. A  $^{152}\text{Eu}$  standard source was used for the energy and efficiency calibration. The resolution of the detector system during counting was 2.0 keV at 1332 keV of  $^{60}\text{Co}$ . Typical gamma ray spectra of irradiated Au and In metal foils are given in Figures 2 and 3, respectively.

From the photo-peak activity ( $A_{\text{obs}}$ ) of the 138.33, 416.86, 818.72, 1097.33 and 1293.56 keV  $\gamma$ -lines of  $^{116m}\text{In}$ , the neutron flux ( $\Phi$ ) was obtained by using Equation (1) from ref. [21]

$$A_{\text{obs}}(\text{CL/LT}) = N\sigma_R\Phi I_\gamma \varepsilon(1 - \exp(-\lambda t)) \times \exp(-\lambda T) \times (1 - \exp(\lambda CL))/\lambda \quad (1)$$

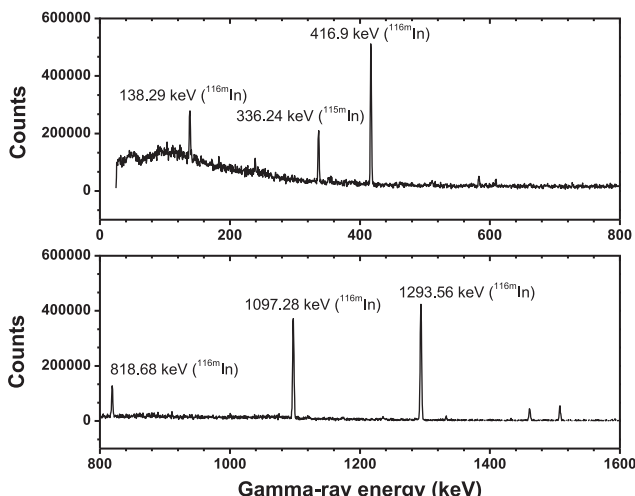


**Fig. 2:** Gamma ray spectrum of irradiated  $^{nat}\text{In}$  foil with the neutron energy of 1.12 MeV; irradiation time = 8.583 h, cooling time = 42 min, and counting time = 10 min.

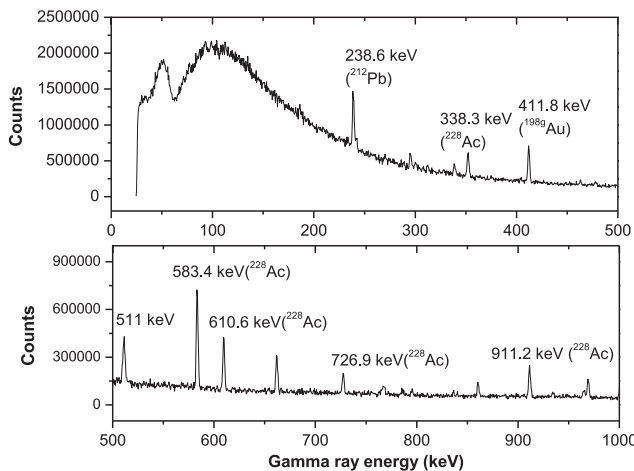


**Fig. 3:** Gamma ray spectrum of irradiated  $^{197}\text{Au}$  foil with the neutron energy of 2.12 MeV; irradiation time = 5.55 h, cooling time = 44.47 h, and counting time = 3.216 h.

where,  $N$  is the number of target atoms and  $\sigma_R$  is the cross-section of the  $^{115}\text{In}(n, \gamma)^{116m}\text{In}$  reaction.  $\lambda$  is the decay constant ( $\lambda = \ln 2/T_{1/2}$ ) of the reaction product of interest with half-life =  $T_{1/2}$ .  $I_\gamma$  is the branching intensity of the 138.33, 416.86, 818.72, 1097.33 and 1293.56 keV  $\gamma$ -line of  $^{116m}\text{In}$  [23] and  $\varepsilon$  is its detection efficiency.  $t$ ,  $T$ , CL and LT are the irradiation time, cooling time, real and live-time of counting, respectively.

The  $^{115}\text{In}(n, \gamma)^{116m}\text{In}$  reaction cross-section is available for a wide range of neutron energies in literature from the work of different authors [24–34]. However, the  $^{115}\text{In}(n, \gamma)^{116m}\text{In}$  reaction cross-sections within the neutron energy range of 1.96 to 7.66 MeV are available in the refs. [29, 31, 32, 34]. Among them, the cross-sections obtained by Husain et al. [31] are within the neutron energy range of 2.44 to 4.5 MeV and are higher than the data of others [29, 32, 34]. Thus the  $^{115}\text{In}(n, \gamma)^{116m}\text{In}$  reaction cross-sections from the refs. [29, 32, 34] were used in the present work for the neutron flux calculation. The evaluated  $^{115}\text{In}(n, \gamma)^{116m}\text{In}$  reaction cross-sections as a function of neutron energy are available in ref. [35]. Thus the neutron flux based on the evaluated  $^{115}\text{In}(n, \gamma)^{116m}\text{In}$  reaction cross-sections were also used to determine the neutron flux. The neutron fluxes obtained from the method described above were used in rearranged Eq. (1) to calculate the  $^{197}\text{Au}(n, \gamma)^{198g}\text{Au}$  reaction cross-section by using the photo-peak activity of the 412.8 keV  $\gamma$ -ray of  $^{198g}\text{Au}$ . The nuclear spectroscopic data used in the above calculations were taken from the ref. [23] and are presented in Table 1. Since the neutron spectrum has some tail, it has effect on the  $^{197}\text{Au}(n, \gamma)^{198g}\text{Au}$  reaction cross-section. At the same time, it also affects the  $^{115}\text{In}(n, \gamma)^{116m}\text{In}$  monitor reaction cross-section. This is

Nuclide	Spin-parity	Half-life	Decay mode	$\gamma$ -ray energy	$\gamma$ -ray abundance (%)
$^{116m}\text{In}$	5 <sup>+</sup>	$54.29 \pm 0.17 \text{ min}$	$\beta^-$ (100%)	138.29	3.7
				416.9	27.2
				818.68	12.13
				1097.28	58.5
				1293.56	84.8
$^{198g}\text{Au}$	2 <sup>-</sup>	$2.6947 \pm 0.0003 \text{ d}$	$\beta^{--}$ (100%)	411.8	95.62

because both the  $^{115}\text{In}(n, \gamma)^{116m}\text{In}$  and  $^{197}\text{Au}(n, \gamma)^{198}\text{Au}$  reaction cross-sections decrease with neutron energy. The contribution in the reaction cross-section due to small tail part is discussed in the next section given below.

### 3 Results and discussion

The  $^{197}\text{Au}(n, \gamma)^{198g}\text{Au}$  reaction cross-sections determined in the present work at the neutron energies of 1.12, 2.12, 3.12 and 4.12 MeV are given in Table 2. The uncertainties associated with the measured cross-section values of present work are from the replicate measurements. The overall uncertainty is the quadratic sum of both statistical and systematic errors. The random error in the observed activity is primarily due to counting statistics, which is estimated to be 3.1%–5.5% for  $^{198g}\text{Au}$ . This can be determined by accumulating the data for an optimum time period that depends on the half-life of the nuclide of interest. The systematic errors are due to uncertainties in the irradiation time (~0.1%), the half-life of the reaction products and the  $\gamma$ -ray abundances (~2%) and the detection efficiency (~3%), which arises from the fitting error. Thus the total systematic error is about ~3.6%. The combined uncertainties from both statistical and systematic errors lie within 4.8%–6.6% for the  $^{197}\text{Au}(n, \gamma)^{198g}\text{Au}$  reaction cross-section. The energy degradation of the pro-

ton beam within the lithium metal foil as well as the  $^{115}\text{In}(n, \gamma)^{116m}\text{In}$  monitor reaction cross-section can cause additional uncertainty. However, this uncertainty is less prominent than the neutron energy uncertainty due to the different extent of population of  $n_0$  and  $n_1$  groups of neutrons.

In order to examine the above aspect, the neutron spectra from the  $^7\text{Li}(p, n)$  reaction at the proton energies of 4, 5 and 6 MeV were calculated as done in our earlier work [21] based on refs. [18–20] and the results are plotted in Figure 4. As mentioned before, the neutron spectrum consists of the full energy peak due to the  $^7\text{Li}(p, n_{0,1})^7\text{Be}$  reaction and a continuum component attributable to the multi-body break up process, i.e.  $^7\text{Li}(p, n^3\text{He})\alpha$  ( $Q = -3.231 \text{ MeV}$ ). This is primarily for the proton energy of 6 MeV but not for 3–5 MeV. However, from the Figure 4, the different extent of population of  $n_0$  and  $n_1$  groups of neutrons, which causes the broadening of the neutron spectrum, can be very well seen. Since the neutron spectrum for the proton energy of 6 MeV has low energy tail, it contributes to the cross-section of the  $^{115}\text{In}(n, \gamma)^{116m}\text{In}$  reaction monitor as well as to the  $^{197}\text{Au}(n, \gamma)^{198g}\text{Au}$  reaction. For this purpose, the  $^{115}\text{In}(n, \gamma)^{116m}\text{In}$  and  $^{197}\text{Au}(n, \gamma)^{198g}\text{Au}$  reaction cross-sections were theoretically calculated by using TALYS 1.6 [17]. This computer code can be used to calculate the reaction cross-section based on physics models and pa-

**Table 1:** Nuclear spectroscopic data of the radionuclides from the  $^{197}\text{Au}(n, \gamma)^{198g}\text{Au}$  and  $^{115}\text{In}(n, \gamma)^{116m}\text{In}$  reactions used in the calculation from Ref. [23]. The bold numbers are the  $\gamma$ -ray energies, whose activities were used in the calculation.

Neutron energy (MeV)	$^{115}\text{In}(n, \gamma)^{116m}\text{In}$		$^{197}\text{Au}(n, \gamma)^{198g}\text{Au}$	
	Cross section (mb)	Flux $\text{n cm}^{-2} \text{s}^{-1}$	Cross section (mb)	Experimental [ref.] TALYS-1.6
1.12 ± 0.12	$174.4 \pm 6.7$ [35]	$(9.421 \pm 0.122) \times 10^6$	$60.441 \pm 3.403$	82.872
1.12 ± 0.12	247.1 [34]	$(6.649 \pm 0.086) \times 10^6$	$85.639 \pm 4.822$	
1.232			$82.5 \pm 3.5$ [12]	
2.12 ± 0.15	$104.1 \pm 4.5$ [35]	$(2.257 \pm 0.155) \times 10^7$	$40.588 \pm 3.063$	79.866
2.12 ± 0.15	129.0 [29]	$(1.821 \pm 0.125) \times 10^7$	$50.306 \pm 3.795$	
2.0			$56.3 \pm 2.4$ [12]	
3.12 ± 0.21	$37.5 \pm 1.5$ [35]	$(2.243 \pm 0.272) \times 10^7$	$19.771 \pm 2.673$	41.255
3.12 ± 0.21	44.6 [32]	$(1.886 \pm 0.229) \times 10^7$	$23.514 \pm 3.182$	
3.0			$25.0 \pm 1.1$ [12]	
4.12 ± 0.32	$15.6 \pm 0.7$ [35]	$(3.062 \pm 0.319) \times 10^7$	$13.944 \pm 1.611$	19.180
4.12 ± 0.32	16.7 [32]	$(2.860 \pm 0.298) \times 10^7$	$14.929 \pm 1.725$	

**Table 2:**  $^{197}\text{Au}(n, \gamma)^{198g}\text{Au}$  and  $^{115}\text{In}(n, \gamma)^{116m}\text{In}$  reaction cross-sections at different neutron energies.

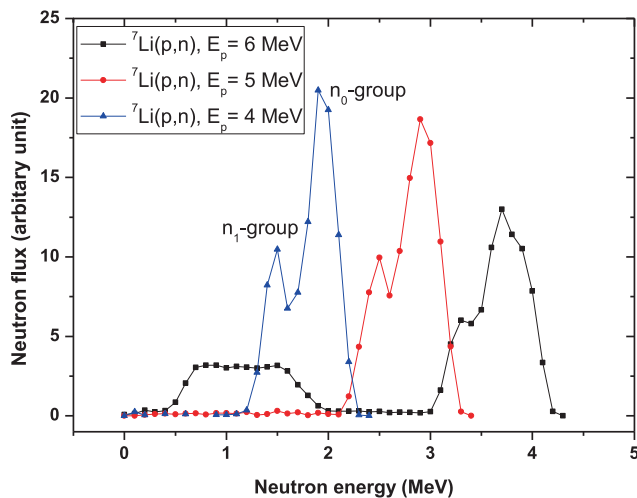


**Fig. 4:** Neutron spectrum from the  $^6\text{Li}(p,n)$  reaction for the proton energy of 6 MeV.

parameterizations. It calculates nuclear reactions involving targets with mass larger than 12 amu and projectiles like photon, neutron, proton,  $^2\text{H}$ ,  $^3\text{H}$ ,  $^3\text{He}$  and alpha particles in the energy range from 1 keV to 200 MeV. In the present work, we did the TALYS calculation by using the default parameters for the neutron energies of 10 keV to 20 MeV with  $^{115}\text{In}$  and  $^{197}\text{Au}$  as targets. All possible outgoing channels for a given projectile (neutron) energy were considered including  $(n,\gamma)$  and inelastic reactions. However, the  $(n,\gamma)$  reaction cross-sections within the neutron energy of 10 keV to 20 MeV were collected. The theoretical reaction cross-sections from TALYS are for the mono-energetic neutrons. Thus the flux-weighted average  $^{115}\text{In}(n,\gamma)^{116m}\text{In}$  and  $^{197}\text{Au}(n,\gamma)^{198g}\text{Au}$  reaction cross-sections ( $\langle \sigma_R \rangle$ ) were calculated using Eq. (2) as given in ref. [21].

$$\langle \sigma_R \rangle = \sum \sigma_R \cdot \varphi / \sum \varphi \quad (2)$$

Using the neutron spectrum of Figure 4 and theoretical values from TALYS, the flux-weighted average  $^{115}\text{In}(n,\gamma)^{116m}\text{In}$  and  $^{197}\text{Au}(n,\gamma)^{198g}\text{Au}$  reaction cross-sections for the neutron energy of 4.12 MeV were obtained as 53.141 and 45.692 mb, respectively. Based on the theoretical flux-weighted average  $^{115}\text{In}(n,\gamma)^{116m}\text{In}$  reaction cross-section of 53.141 mb and the photo-peak activity of 412.8 keV  $\gamma$ -ray of  $^{198g}\text{Au}$ , the  $^{197}\text{Au}(n,\gamma)^{198g}\text{Au}$  reaction cross-section was obtained as 47.506 mb. This is close to the theoretical flux-weighted average  $^{197}\text{Au}(n,\gamma)^{198g}\text{Au}$  reaction cross-section of 45.692 mb. Thus for the neutron energy of 4.12 MeV, the experimental  $^{115}\text{In}(n,\gamma)^{116m}\text{In}$  reaction cross-section of 16.7 mb [32] and the photo-peak activity of 412.8 keV  $\gamma$ -ray of  $^{198g}\text{Au}$ , the  $^{197}\text{Au}(n,\gamma)^{198g}\text{Au}$

reaction cross-section obtained as 14.926 mb is reasonable. This is because both the  $^{115}\text{In}(n,\gamma)^{116m}\text{In}$  and  $^{197}\text{Au}(n,\gamma)^{198g}\text{Au}$  reaction cross-sections decrease in parallel with increase of neutron energy. Thus the contribution to the  $^{197}\text{Au}(n,\gamma)^{198g}\text{Au}$  reaction cross-section due to the tail part of the neutron spectrum has been avoided by using the  $^{115}\text{In}(n,\gamma)^{116m}\text{In}$  reaction cross-section as the neutron flux monitor. Based on the above argument, the  $^{197}\text{Au}(n,\gamma)^{198g}\text{Au}$  reaction cross-section shown in Table 2 using the experimental  $^{115}\text{In}(n,\gamma)^{116m}\text{In}$  reaction cross-section at the neutron energies of 1.12–4.12 MeV are reasonable. For the proton energies of 3, 4 and 5 MeV, the neutron spectra have no tail part of the neutrons. Thus the  $^{197}\text{Au}(n,\gamma)^{198g}\text{Au}$  reaction cross-section at the neutron energies of 1.12, 2.12 and 3.12 MeV does not need the corrections.

The  $^{197}\text{Au}(n,\gamma)^{198g}\text{Au}$  reaction cross-sections at the neutron energies of 1.12, 2.12, 3.12 and 4.12 MeV were determined in the present work for the first time. There is no data available in literature [5–16] within the neutron energy range of 3–4.5 MeV. However, data at the neutron energy of 0.025 eV [1–3], within 0.2–3 MeV [7–13, 16] and at 14.7 MeV [14, 15] are available in literature. The experimental data of present work at the neutron energies of 1.12 and 2.12 MeV lie in between the values within the neutron energies of 1 to 1.2 MeV and 2 to 2.2 MeV, respectively. However, for all four neutron energies, the  $^{197}\text{Au}(n,\gamma)^{198g}\text{Au}$  reaction cross-sections based on the evaluated  $^{115}\text{In}(n,\gamma)^{116m}\text{In}$  reaction cross-sections [35] are lower than the experimental values. In view of this, the theoretical  $^{197}\text{Au}(n,\gamma)^{198g}\text{Au}$  reaction cross-sections from TALYS 1.6 at the neutron energies of 1.12, 2.12, 3.12 and 4.12 MeV are shown in Table 2 for comparison.

It can be seen from Table 2 that the experimentally determined reaction cross-sections from the present work at the neutron energies of 1.12 and 4.12 are in general agreement with the theoretical values of TALYS 1.6 [17]. However, the data at the neutron energies of 2.12 and 3.12 MeV are lower than the theoretical values of TALYS 1.6. It can be also seen from Table 2 that the  $^{197}\text{Au}(n,\gamma)^{198g}\text{Au}$  reaction cross-sections based on the evaluated  $^{115}\text{In}(n,\gamma)^{116m}\text{In}$  reaction cross-sections are very much lower than the theoretical values of TALYS 1.6. The experimental data from the present work at the four neutron energies and literature data [3–16] at other neutron energies along with the theoretical values from TALYS 1.6 within the 10 keV to 20 MeV are plotted in Figure 5. It can be seen that the experimental data from the present work and the literature data [7–13] within the neutron energies of 2.12–4.12 MeV are slightly lower than the theoretical values but follow a similar trend closely. The  $^{197}\text{Au}(n,\gamma)^{198g}\text{Au}$  reaction

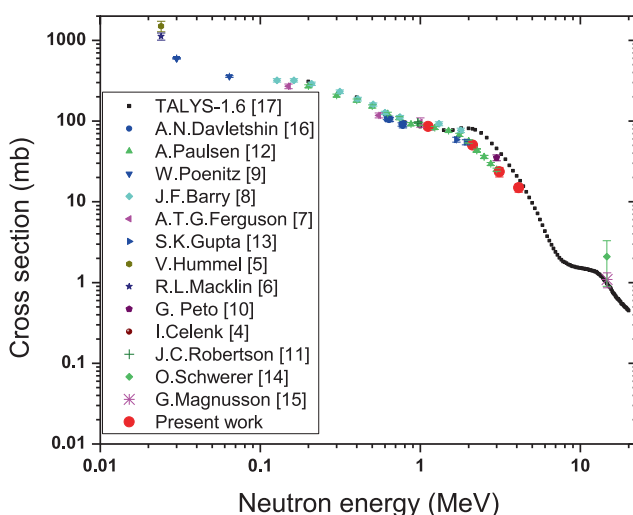


**Fig. 5:** Plot of the experimental and theoretical  $^{197}\text{Au}(n,\gamma)^{198\text{g}}\text{Au}$  reaction cross-section as a function of the neutron energy from 10 keV to 20 MeV. Experimental values from the present work and from Refs. [3–16] are in different symbols and colour, whereas the theoretical values from TALYS are in solid square.

cross-section at different neutron energies is important from the point of view of its use for the determination of neutron flux during other reaction cross-section measurements. It is a well-known fact that the  $^{197}\text{Au}(n,\gamma)^{198\text{g}}\text{Au}$  reaction cross-section as a function of neutron energy is one among the nine of the IAEA standard reaction monitors. Based on the IAEA reaction cross-section standards, the uncertainties for the neutron capture cross-section of Au should be within 1.4%–2.2%. Since we did the measurements of  $\text{Au}(n,\gamma)$  reaction cross-section based on the experimental  $^{115}\text{In}(n,\gamma)^{116\text{m}}\text{In}$  reaction cross section, the uncertainty is on the higher side. This can be mentioned by the evaluator. Besides this, the experimentally determined  $^{197}\text{Au}(n,\gamma)^{198\text{g}}\text{Au}$  reaction cross-section is important for the test of TALYS model.

## 4 Conclusions

We determined the  $^{197}\text{Au}(n,\gamma)^{198\text{g}}\text{Au}$  reaction cross-section at the neutron energies of 1.12, 2.12, 3.12 and 4.12 MeV by using an activation and off-line  $\gamma$ -ray spectrometric technique. The values for the latter two energies are reported for the first time. Our data at the neutron energies of 1.12 and 2.12 MeV are in agreement with the literature data. The  $^{197}\text{Au}(n,\gamma)^{198\text{g}}\text{Au}$  reaction cross-section as a function of neutron energy was also calculated theoretically using the computer code TALYS 1.6 version. The present data at four neutron energies and the literature

data at other neutron energies are systematically lower than the theoretical values.

**Acknowledgement:** One of the authors (V. Vansola) thanks the staff of the folded tandem ion beam accelerator (FOTIA) at Van-de-Graaff, BARC and Pelletron facility, TIFR for their excellent operation of the accelerator and giving the proton beam during the irradiation.

## References

- Carlson, A. D., Pronyaev, V. G., Smith, D. L., Larson, N. M., Chen, Zhenpeng., Hale, G. M., Hambisch, F.-J., Gai, E. V., Oh, Soo-Youl, Badikov, S. A., Kawano, T., Hofmann, H. M., Vonach, H., Tagesen, S.: International Evaluation of Neutron Cross Section Standards. *Nucl. Data Sheets* **110**, 3215–3324 (2009).
- IAEA-EXFOR Database, available at <http://www-nds.iaea.org/exfor>.
- Antonini, D., Moioli, P., Pedretti, E., Scafe, R., Isentin, A.: Measurements of activation cross sections by generalized intermittent radiation. *Nucl. Instrum. Meth. In Phys. Res.* **115**, 567–572 (1978).
- Celenk, I., Demirel, H., Ozmen, A.: Measurement of Macroscopic and Microscopic Thermal Neutron Cross Sections of V, Co, Cu, In, Dy and Au using Neutron Self-Absorption Properties. *J. Radioanal. Nucl. Chem.* **148**, 393–401 (1991).
- Hummel, V., Hamermesh, B.: Activation cross sections measured with antimony-beryllium neutrons. *Phys. Rev.* **82**, 67–68 (1951).
- Macklin, R. L., Lazar, N. H., Lyon, W. S.: Neutron Activation Cross Sections with Sb–Be Neutrons. *Phys. Rev.* **107**, 504–508 (1957).
- Ferguson, A. T. G., Paul, E. B.: The capture cross section of Au-197 for fast neutrons. *J. Nucl. Energy A (Reactor Science)* **10**, 19–21 (1959).
- Barry, J. F.: The radiative capture cross section of Au-197 for neutrons in the energy range 0.12–1.8 MeV. *J. Nucl. Energy A & B (Reactor Sci. and Tech.)* **18**, 491–496 (1964).
- Poenitz, W.: The  $(n,\gamma)$  cross-section of Au-197 at 30 and 64 keV neutron energy. *J. Nucl. Energy A & B (Reactor Sci. and Techn.)* **20**, 825–834 (1966).
- Peto, P., Milligay, Z., Hunyadi, I.: Radiative capture cross-sections for 3 MeV neutrons. *J. Nucl. Energy* **21**, 797–801 (1967).
- Robertson, J. C., Ryves, T. B., Axton, E. J., Goodier, I., Williams, A.: A Measurement of the adiabatic Capture Cross Section of Gold at an Energy of 966 keV. *J. Nucl. Energy* **23**, 205–210 (1969).
- Paulsen, A., Widera, R., Liskien, H.: Au197(n,g)Au198 cross-section measurements between 0.2 and 3.0 MeV. *Atomkernenergie* **26**, 80 (1975).
- Gupta, S. K., Frehaut, J., Bois, R.: Radiative capture cross section measurements for fast neutrons using a large Gd-loaded liquid scintillator. *Nucl. Instrum. Meth. in Phys. Res.* **148(1)**, 77–84 (1978).

14. Schwerer, O., Winkler-Rohatsch, M., Warhanek, H., Wikler, G.: Measurement of cross sections for 14 MeV neutron capture. *Nucl. Phys. A* **264**, 105–114 (1976).
15. Magnusson, G., Andersso, P., Bergqvist, I.: 14.7 MeV Neutron Capture Cross-Section Measurements with Activation Technique. *Phys. Scripta* **21**, 21–26 (1980).
16. Davletshin, A. N., Korytchenko, V. N., Tipunkov, A. O., Tikhonov, S. V., Tolstikov, V. A.: Cross Section for Radiative Capture of Neutrons by  $^{197}\text{Au}$ . An Analysis of Sources of Systematic Errors in Measurement of Activation. *Atomic Energy* **65**(5), 913–919 (1988).
17. Koning, A. J.: TALYS user manual, A nuclear reaction program, User manual NRG-1755 ZG PETTEN, The Netherlands, 2011.
18. Liskien, H., Paulsen, A.: Neutron production cross sections and energies for the cross sections  $^7\text{Li}(p,n)^7\text{Be}$  and  $^7\text{Li}(p,n)^7\text{Be}^*$ . *At. Data Nucl. Data Tables* **15**, 57–84 (1975).
19. Poppe, C. H., Anderson, J. D., Davis, J. C., Grimes, S. M., Wong, C.: Cross sections for the  $\text{Li}7(p,n)\text{Be}7$  reaction between 4.2 and 26 MeV. *Phys. Rev. C* **14**, 438–445 (1976).
20. Meadows, J. W., Smith D. L.: Neutrons from proton bombardment of natural Lithium, Argonne National Laboratory Report ANL-7983, 1972.
21. Naik, H., Prajapati, P. M., Surayanarayana, S. V., Jagadeesan, K. C., Thakare, S. V., Raj, D., Mulik, V. K., Sivashankar, B. S., Nayak, B. K., Sharma, S. C., Mukherjee, S., Singh S., Goswami, A., Ganesan S., Manchanda, V. K.: Measurement of the neutron reaction cross-section of  $^{232}\text{Th}$  using the neutron activation Technique. *Eur. Phys. J. A.* **47**(51) 1–9 (2011).
22. Ziegler, J. F.: SRIM-2003. *Nucl. Instrum. Methods Phys. Res., Sect. B, Beam Interact.* **219–220**, 1027–1036 (2004), available at <http://www.srim.org/>.
23. NuDat 2.6, National Nuclear Data Center, Brookhaven National Laboratory, updated 2011, available at <http://www.nndc.bnl.gov/>.
24. Grench, H. A., Menlove, H. O.:  $\text{In}113(n,\gamma)\text{In}114m$ ,  $\text{In}113(n,n'\gamma)\text{In}113m$ ,  $\text{In}115(n,\gamma)\text{In}116m$ ,  $116g$ , and  $\text{In}115(n,n')\text{In}115m$  Activation Cross Sections between 0.36 and 1.02 MeV. *Phys. Rev.* **165**, 1298–1311 (1968).
25. Ponnert, K., Magnusson, G., Bergqvist, I.: Multiple Reaction Correction to 15 MeV Neutron Capture Cross Section in  $^{115}\text{In}$ . *Phys. Scripta* **10**, 35–41 (1974).
26. Peto, G., Csikai, J., Long, V., Mukherjee, S., Banhalmi, J., Miligy, Z.: Radiative capture cross-sections for 14.7 MeV neutrons. *Acta Phys. Slovaca*, **25**, 185–189 (1975).
27. Mannhart, W.: Thermal neutron activation cross sections with high accuracy-ger. *Zeitschrift fuer Physik A, Hadrons and Nuclei* **272**, 273–277 (1975).
28. Magnusson, G., Bergqvist, I.: 14.7-MeV neutron capture cross-section measurements with improved activation technique. *Nucl. Tech.* **34**, 114–121 (1977).
29. Andersson, P., Zorro, R., Bergqvist, I.: On neutron capture cross section measurements with the activation technique in the MeV region. *Conf. on Nucl. Data for Sci. And Technol.*, Bockhoff, K. H. (editor), Antwerp, Belgium, Sept. 6–10, Page 866, 1982, Published by D. Reidel Publishing Company, P. O. Box 17, 3300 AA Dordrecht, Holland.
30. Demekhin, V. L., Leshchenko, B. E., Majdanuk, V. K., Peto, G.: 14.6 MeV neutron radiation capture cross-section determination for In-115. Sixth All-Union Conf. On Neutron Physics, Vol. 3, Kiev, 2–6 Oct., 195 (1983).
31. Husain, H. A., Hunt, S. E.: Absolute Neutron Cross Section Measurements in the Energy Range between 2 and 5 MeV. *Int. J. Applied Radiation and Isotopes* **34**, 731–738 (1983).
32. Andersson, P., Zorro, R., Berqvist, I., Herman, M., Marcinkowski, A.: Cross Sections for  $^{197}\text{Au}(n,\gamma)^{198}\text{Au}$  and  $^{115}\text{In}(n,\gamma)^{116m}\text{In}$  in the Neutron Energy Region 2.0–7.7 MeV. *Nucl. Phys. A* **443**, 404–414 (1985).
33. Grady, D. J., Knoll, G. F., Robertson, J. C.: Absolute Measurements of the  $^{115}\text{In}(n,\gamma)^{116m}\text{In}$  Cross Section for Fast Neutrons. *Nucl. Sci. Eng.*, **94**, 227–232 (1986).
34. Gautam, R. P., Singh, R. K., Rizvi, I. A., Afzal Ansari, M., Chaubey, A. K., Kailas, S.: Measurement of radiative capture of fast neutrons in Mn-55 and In-115. *Indian J. Pure and Applied Phys.* **28**, 235 (1990).
35. Zolotarev, K. I., Zolotarev, P. K.: Evaluation of the excitation functions for the  $^{54}\text{Fe}(n,p)^{54}\text{Mn}$ ,  $^{58}\text{Ni}(n,2n)^{57}\text{Ni}$ ,  $^{67}\text{Zn}(n,p)^{67}\text{Cu}$ ,  $^{92}\text{Mo}(n,p)^{92m}\text{Nb}$ ,  $^{93}\text{Nb}(n,\gamma)^{94}\text{Nb}$ ,  $^{113}\text{In}(n,n')^{113m}\text{In}$ ,  $^{115}\text{In}(n,\gamma)^{116m}\text{In}$ , and  $^{169}\text{Tm}(n,3n)^{167}\text{Tm}$  reactions. Progress Report on Research Contract No 16242, INDC(NDS)-0657, December 2013, available at <https://www-nds.iaea.org/publications/indc/indc-nds-0657.pdf>.